Available online at www.sciencedirect.com

ScienceDirect

Journal of the Chinese Medical Association 78 (2015) 218–228

www.jcma-online.com

Original Article

Comparative proteomic analysis of rat left ventricle in a subtotal nephrectomy model

Yao-Ping Lin [a,b], Wen-Chung Yu [a,b], Meng-Erh Hsu [b], Hsiao-Chien Tsai [b], Chen-Chung Liao [c,*], Chao-Hsiung Lin [c,d,e,f]

[a] *National Yang-Ming University School of Medicine, Taipei, Taiwan, ROC*
[b] *Department of Medicine, Taipei Veterans General Hospital, Taipei, Taiwan, ROC*
[c] *Proteomics Research Center, National Yang-Ming University, Taipei, Taiwan, ROC*
[d] *Department of Medical Research and Education, Taipei Veterans General Hospital, Taipei, Taiwan, ROC*
[e] *Department of Education and Research, Taipei City Hospital, Taipei, Taiwan, ROC*
[f] *Department of Life Sciences and Institute of Genome Sciences, National Yang-Ming University, Taipei, Taiwan, ROC*

Received August 6, 2014; accepted August 25, 2014

Abstract

Background: Chronic kidney disease (CKD) is associated with cardiac hypertrophy that leads to increased cardiovascular morbidity and mortality. To date, use of the renin–angiotensin–aldosterone system blockade has been the main treatment modality. However, renin–angiotensin–aldosterone system blockade by the angiotensin converting enzyme inhibitors (ACEi) can only partially reverse the cardiac hypertrophy without having a significant impact on all-cause mortality as evidenced by meta-analyses from clinical trials. It is imperative to elucidate the molecular pathogenesis of CKD-related cardiomyopathy for potential targets in further treatment.

Methods: Male Sprague–Dawley rats that underwent subtotal nephrectomy (SNX) rats were established as the CKD model. A hemodynamic study was used to evaluate the left ventricle (LV) structural and functional alterations. We used proteomic techniques to profile the LV protein changes among sham-operated rats, SNX rats, and SNX rats with 6 months of ACEi enalapril interventions. The differentially expressed proteins were further annotated by functional and network analyses.

Results: As compared to the sham-operated rats, the SNX rats had 25 upregulated and 46 decreased protein expression. The top canonical pathways identified by ingenuity pathway analysis for the CKD cardiomyopathy were mitochondrial dysfunction, oxidative phosphorylation, fatty acid β oxidation, protein ubiquitination, and ketolysis. The most relevant functions extracted from these networks contained 27 and 23 focused proteins, respectively. They were related to cellular assembly and organization, RNA posttranscriptional modification, and protein synthesis. After ACEi intervention for 6 weeks, the residual canonical pathways identified by ingenuity pathway analysis that mediated the CKD-related cardiomyopathy were mitochondrial dysfunction, ketolysis, phenylalanine degradation IV, and putrescine degradation III. There were decreased Sirt3 and SNRNP, and increased monoamine oxidase and SAHH expression in the LV of SNX rats that could not be reversed by the ACEi.

Conclusion: Our studies provide a repertoire of potential biomarkers related to cardiac hypertrophy in CKD. There are still residual disturbed molecules/pathways despite ACEi intervention. Further studies are warranted to investigate these potential novel targets to alleviate CKD-related cardiomyopathy.

Keywords: angiotensin converting enzyme inhibitor; chronic kidney disease; hemodynamics; left ventricular hypertrophy; proteomics

Conflicts of interest: The authors declare that there are no conflicts of interest related to the subject matter or materials discussed in this article.

* Corresponding author. Dr. Chen-Chung Liao, Proteomics Research Center, National Yang-Ming University, 155, Section 2, Li-Nong Street, Taipei 112, Taiwan, ROC.

E-mail address: ccliao@ym.edu.tw (C.-C. Liao).

http://dx.doi.org/10.1016/j.jcma.2014.08.016

1. Introduction

The prevalence of chronic kidney disease (CKD) is expanding rapidly worldwide. Although enormous efforts have been devoted to alleviate renal function deterioration, cardiovascular disease remains the main cause of morbidity and mortality in this population.

Contrary to the multitude of randomized control trials (RCTs) for cardiovascular diseases in the general population, there are still limited studies specifically designed for CKD-related cardiac dysfunctions.[1] RCTs for cardiovascular diseases often exclude renal impairment patients at the very beginning of enrollment. Nevertheless, for the few RCTs of renal diseases that have been reported, they seldom considered cardiovascular parameters as the composite end point for analysis.[2] Therefore, current treatment strategies toward CKD-related cardiovascular disease have mainly been derived from experience with nonrenal dysfunction patients. It should be noted that besides the traditional cardiovascular risk factors, there are specific uremia-related milieus that contributed to the cardiovascular pathology. Without a comprehensive understanding of the molecular signatures and pathways, it would be impossible to develop specific therapeutic interventions for this CKD-related cardiac dysfunction.

Because CKD is well known for the uncontrolled activation of renin–angiotensin–aldosterone system (RAAS), RAAS blockade [e.g., ACE inhibitors (ACEi) by enalapril] has been the mainstay cardiovascular treatment modality.[3] However, a recent Cochrane review of four RCTs that enrolled 2177 stage 1–3 nondiabetic CKD patients suggested that ACEi had no impact on all-cause mortality.[4] For those CKD 5 patients under maintenance hemodialysis, the secondary analysis of the RCT of HEMO (originally targeted toward dialysis dose and membrane flux) also revealed that ACEi could not significantly affect mortality or cardiovascular morbidity,[5] and even unexpectedly had a higher risk of heart failure hospitalization. When taking left ventricular mass (LVM) as the surrogate marker, Dyadyk et al[6] reported that ACEi (captopril and enalapril) could only induce regression in 12–19% of LVM in hypertensive CKD patients. Our previous 12-month RCT with the ACEi ramipril also failed to render significant regression of LVM in normotensive hemodialysis patients.[7] Therefore, it is imperative to elucidate mechanisms beyond RAAS that mediate the pathogenesis of uremic cardiomyopathy.

Proteomic techniques have been adopted to investigate cardiovascular biology.[8] However, there is still scarce application of these techniques to study CKD-related cardiomyopathy. In this study, we used advanced proteomic techniques to unravel the molecular signatures of uremic-related cardiomyopathy, and to search for the remaining pathological pathway/molecules after RAAS blockade by ACEi treatment. We endeavored to improve our incomplete understanding of the pathophysiology of CKD-related cardiomyopathy and explore the potential candidate targets for therapeutic interventions.

2. Methods

2.1. Rat subtotal nephrectomy model

This study was conducted according to the guidelines of the Taipei Veterans General Hospital Committee on Animal Care and Supply, Taipei, Taiwan. Male Sprague–Dawley rats (from National Laboratory Animal Center, Taipei, Taiwan) (200–250 g) were housed in animal care facilities with living conditions maintained as follows: 12-hour light/dark cycles, temperature at 21°C, and humidity at 70%. The rats were randomly allocated into three groups: sham-operated (SO), subtotal nephrectomy (SNX) with vehicle (corn oil), and SNX with the ACEi enalapril (3 mg/kg/d). The rat SNX models were established similar to that in previous studies by removing one kidney and two-thirds of the remaining kidney at two stages.[9] The SO group received two-stage bilateral renal decapsulation. After the surgical procedures were completed, the rats were gavaged with either vehicle or enalapril for 6 weeks. All rats were provided standard food (containing 40 g protein and 0.6 g NaCl per 100 g) and tap water *ad libitum*.

2.2. Hemodynamic study

The rats were anesthetized with intraperitoneal pentobarbital sodium (40 mg/kg body weight). During the procedure, the rat's body temperature was maintained at 37°C with a small animal blanket. The neck was carefully dissected to isolate the right carotid artery, through which a 1.9F conductance catheter (Scisense FT212, Ontario, Canada) was introduced into the ascending aorta. The systolic and diastolic blood pressures of the rats were then recorded to represent the central blood pressure.

Subsequently, the conductance catheter was advanced into the left ventricle (LV) to obtain the left ventricle hemodynamic parameters. The heart rate, LV end-systolic pressure, LV end-diastolic pressure, LV end-systolic volume, and LV end-diastolic volume were recorded. The systolic function are indexed by ejection fraction, peak positive value of the time derivative of LV pressure (dP/dt_{min}), and cardiac output, which is derived from (stroke volume) × (heart rate). The diastolic function parameters are represented by the peak negative value of the time derivative of LV pressure (dP/dt_{min}) and isovolumetric relaxation constant (microseconds).

2.3. Preparation of crude tissue extracts

After the hemodynamic study, the rats were sacrificed via an intraperitoneal injection of superdose sodium pentobarbital. Each heart was harvested, perfused with phosphate-buffered saline, and weighed, after which the left ventricles were further dissected. For each rat, 100 mg of the left ventricle was minced and treated with 500 μL of extraction buffer [0.5 M Tris, pH 6.8, 0.1% sodium dodecyl sulfate (SDS)] containing the complete protease inhibitor cocktail (Roche, Mannheim, Germany) and PhosSTOP phosphatase inhibitor cocktail

Table 1
Characteristics and hemodynamic data of the sham-operated, subtotal nephrectomy + vehicle, and subtotal nephrectomy + enalapril rats.

Parameters	Sham-operated ($N = 6$)	Subtotal nephrectomy + Vehicle ($N = 6$)	Subtotal nephrectomy + Enalapril ($N = 6$)
Body weight (g)	420 ± 35	390 ± 39	397 ± 42
Renal function indices			
Blood urea nitrogen (mg/dL)	16.2 ± 1.4	45.3 ± 2.8*	36.2 ± 3.1*,**
Creatinine (mg/dL)	0.8 ± 0.0	1.4 ± 0.1*	1.2 ± 0.1*,**
Carotid systolic blood pressure (mmHg)	116.7 ± 12.5	168.5 ± 14.6*	132.4 ± 11.8*,**
Carotid diastolic blood pressure (mmHg)	76.8 ± 13.1	106.5 ± 11.7*	94.2 ± 12.4*,**
Heart weight/body weight (%)	0.27 ± 0.02	0.38 ± 0.02*	0.32 ± 0.01*
Heart rate (/min)	382 ± 21	373 ± 29	360 ± 23
Left ventricular systolic pressure (mmHg)	156.9 ± 11.3	177.4 ± 28.0*	148.6 ± 12.4**
Left ventricular end diastolic pressure (mmHg)	17.4 ± 2.3	16.1 ± 4.2	15.5 ± 0.8
Ejection fraction (%)	56.3 ± 11.9	52.0 ± 9.3	54.3 ± 10.4
Cardiac output (mL/min)	50.6 ± 4.5	53.4 ± 7.9	52.0 ± 6.6
dP/dt_{max} (mmHg/s)	8974 ± 436	8592 ± 1067	7810 ± 1198
dP/dt_{min} (mmHg/s)	6335 ± 575	5767 ± 900*	5986 ± 724*,**
Isovolumetric relaxation time (ms)	14.3 ± 0.6	17.5 ± 1.3*	15.2 ± 0.8

Data are expressed as mean ± standard error.
*$p < 0.05$ compared to sham-operated rats.
**$p < 0.05$ compared to subtotal nephrectomy + vehicle rats.
dP/dt_{max} = maximum derivative of change in systolic pressure over time; dP/dt_{min} = maximum derivative of change in diastolic pressure over time.

(Roche). Then, each sample was homogenized individually and centrifuged at 20,630*g* for 30 minutes at 4°C (Model 5922; Kubota Corp., Tokyo, Japan) to remove cell debris. The supernatants were collected, and total protein concentrations were determined using the protein assay rapid kit (Wako Pure Chemical Industries, Osaka, Japan).

2.4. SDS-polyacrylamide gel electrophoresis and in-gel digestion

Rat left ventricular protein samples were fractionated by 10% SDS-polyacrylamide gel electrophoresis, similar to a previously described method.[10] The gels were stained with CBB staining solution (0.1% CCBG-250, 34% methanol, 17% ammonium sulfate, and 3% *O*-phosphoric acid), and 50 μg of each protein sample was loaded onto the gel in triplicate. The gel lanes were cut into 10 fractions based on molecular weight, and the gel slices were destained repeatedly in a solution of 25 mM NH_4HCO_3 and 50% (v/v) acetonitrile (1:1). After drying in a Speed-Vac (concentrator 5301; Eppendorf AG, Hamburg, Germany), the slices were incubated with 1% β-mercaptoethanol and 25 mM NH_4HCO_3 for 20 minutes at room temperature. For cysteine alkylation, an equal volume of 5% 4-vinylpyridine in 25 mM NH_4HCO_3 and 50% acetonitrile was added for 20 minutes. After soaking the slices in 1 mL 25 mM NH_4HCO_3 for 10 minutes, the slices were dried in a Speed-Vac for 20 minutes. Then, 200 ng of modified trypsin (Promega, Mannheim, Germany) in 25 mM NH_4HCO_3 was added, and tryptic digestion was performed at 37°C overnight. The tryptic digest was removed from the gel, dried in a Speed-Vac, and stored at −20°C until further analysis. The tryptic peptides were resuspended in 20 μL 0.1% (v/v) formic acid immediately before use.

2.5. Mass spectrometric analysis

Tryptic peptide samples were injected into a nanoflow HPLC system (Agilent Technologies 1200 series; Agilent Technologies, Waldbronn, Germany) coupled to an LTQ-

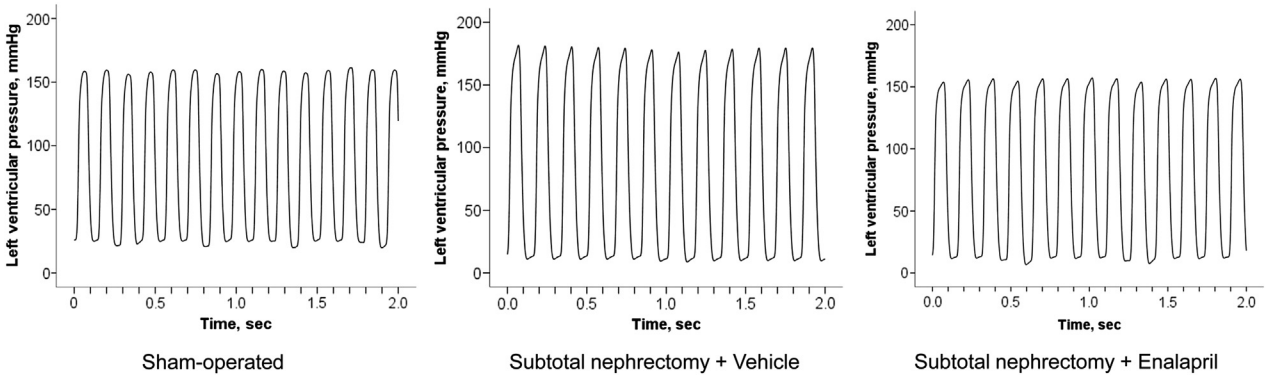

Fig. 1. Representative left ventricular pressure recordings of the sham-operated rats, subtotal nephrectomy rats treated with vehicle, and subtotal nephrectomy rats treated with enalapril. Compared to sham-operated controls, the SNX rats have significantly higher left ventricular systolic pressure, which could be lowered by enalapril treatment. SNX = subtotal nephrectomy.

Orbitrap Discovery hybrid mass spectrometer with a nano-electrospray ionization source (Thermo Electron, Waltham, MA, USA). The tryptic peptides were separated on an Agilent C18 column (100 mm × 0.075 mm, particle size 3.5 μm). Mobile-phase solvent A was prepared as 0.1% formic acid in water, and solvent B as 0.1% formic acid in acetonitrile. The peptides were eluted from the column with a linear gradient of 5–35% solution B for 90 minutes and 35–95% solution B for 10 minutes. The eluted peptides were ionized with a spray voltage of 2 kV and then introduced into the mass spectrometer (MS). MS data were obtained using the data-dependent acquisition method (isolation width: 1.5 Da), in which one full MS survey scan ($m/z = 200–2000$) at a high resolution of 30,000 at full-width half maximum was followed by a tandem mass spectrometry (MS/MS) scan of the six most intense ions with 2^+ and 3^+ charge states. Fragment ions of each selected precursors were generated by collision-induced dissociation using helium gas with collision energy of 35 eV.

2.6. Database searching

The LC-MS/MS raw data were analyzed using the Xcalibur 2.0.7 SR1 software (Thermo Electron), processed by an in-house server where the peptide sequences were identified against the Universal Protein Resource Knowledgebase, a rat protein database (UniProt; http://www.uniprot.org/) that contains ion scans obtained from MS/MS data. The lists of searching parameters were set as follows: peptide mass tolerance of 1.0 Da; fragment ion tolerance of 1.5 Da, enzyme designated as trypsin; one missed cleavage by trypsin was allowed; oxidation on methionine (+16 Da) was allowed as variable modifications. Positive protein identification was based on the following criteria for an assigned peptide as Xcorr ≥2.2 for 2^+, and 3.75 for 3^+ charged ions. A protein was considered to be identified when at least two peptides were matched with the above Xcorr scores. MS spectral counts were normalized on the sum of the spectral counts per biological sample for quantitative analyses.

2.7. Pathway analysis

The differentially expressed left ventricular proteins between SO and SNX + vehicle, and those between SNX + vehicle and SNX + enalapril were uploaded with their corresponding Swiss-Prot accession numbers into the ingenuity pathway analysis (Ingenuity Systems, www.ingenuity.com) for networks and functional analyses.

2.8. Western blotting

Frozen left ventricle tissues were pulverized into a fine powder under liquid nitrogen, dissolved in a lysis buffer (9.5 M urea, 2% w/v CHAPS. 0.8% w/v Pharmalyte, pH 3–10 and 1% w/v DTT) containing protease inhibitors, and then centrifuged at 20,630*g* for 10 minutes. The supernatant were collected and the protein concentration determined by use of the Bradford method (Bio-Rad, Hercules, California, USA).

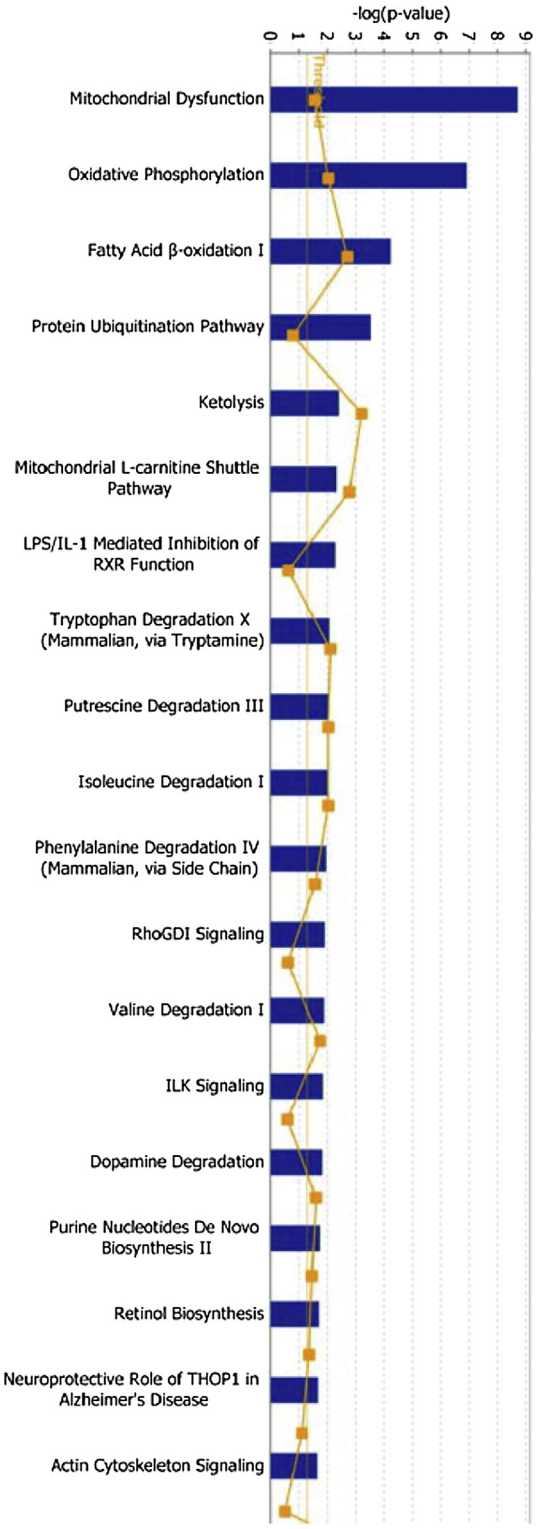

Fig. 2. Predominant canonical pathway identified by ingenuity pathway analysis for the differentially expressed left ventricular proteins between sham-operated rats and the subtotal nephrectomy rats treated with vehicle. The top canonical pathways participated in the CKD cardiomyopathy were mitochondrial dysfunction, oxidative phosphorylation, fatty acid β oxidation, protein ubiquitination, and ketolysis. CKD = chronic kidney disease.

Samples with equal protein amounts were fractionated on 10% SDS-polyacrylamide gel electrophoresis, then transferred to polyvinylidene difluoride membranes. After the membrane was blocked with the blocking solution (5% skim milk), it was incubated with the primary antibodies as SirtT3 (Cell Signaling), SNRNP200 (Abnova), Monoamine Oxidase A and SAHH (Santa Cruz Biotechnology, Santa Cruz, CA, USA) at 4°C overnight. The membrane was subsequently incubated with peroxidase-conjugated secondary antibody. After washing, the blots were visualized using the enhanced chemiluminescence method, and ImageJ software was used to quantify the image signal.

2.9. Statistical analysis

Data are expressed as mean ± SE. All statistical analyses were conducted using SPSS, version 19.0 (SPSS Inc., Chicago, IL, USA). Unpaired Student *t* test was conducted for comparisons between groups, and analysis of variance was used for comparisons among groups. A p value <0.05 was considered statistically significant.

3. Results

3.1. Biochemical and hemodynamic data

Blood and urine measurements for each SO, SNX + vehicle, and SNX + ACEi rat were performed every 2 weeks to ensure a successful establishment of the animal model and monitor treatment effects. As demonstrated in Table 1, the SNX rats had significantly more impaired renal function indexed by increased blood urea nitrogen and creatinine than the SO rats. However, 6 weeks of enalapril treatment could partially improve the renal function. The SNX rats had markedly higher carotid systolic and diastolic blood pressure, and enalapril could lower the blood pressure. The SNX fed with vehicle had a significant hypertrophic heart as indicated by the increased heart weight/body weight ratio.

Table 2
Ingenuity pathway analysis of the differentially expressed left ventricular proteins in the subtotal nephrectomy rats treated with vehicle when compared with the sham-operated rats.

ID	Molecules in network[a]	Score[b]	Focus molecule	Top diseases and functions
1	↓ACAA2, ↓ACADM, ↓AFM, Akt, ↑ALDH2, ↓ECHS1, estrogen receptor, ↓ETFA, ↓FHL1, ↓FHL2, Growth hormone, ↑GSTM1, ↓HBA1/HBA2, hemoglobin, ↓HK2, ↓LAMA4, ↓LOC299282, ↓LONP1, ↑MAOA, mitochondrial complex 1, ↓MT-CO2, ↓MT-ND1*, NADH2 dehydrogenase, ↓NAMPT, ↑NDUFA2, ↓NDUFA4, ↓NDUFA11, ↑NDUFV1, ↑NDUFV2, PDGF BB, ↑SERPINA3, ↓SERPINB6, ↑SERPINF1, ↓SIRT3, trypsin	61	27	Developmental disorder, hereditary disorder, metabolic disease
2	**↑AHCY**, Ap1, CD3, Ck2, **↓ENO3**, **↓FABP3**, **↓FKBP3**, **↑GDI1**, **↓GDI2**, **↑HBB***, Histone h3, **↓HNRNPA2B1**, **↓HSPA8***, IgG, Insulin, **↓KIF5B**, **↓KPNA4**, **↓MYO1C**, NFkB (complex), p85 (pik3r), **↓PAFAH1B2**, Pkc(s), **↓PNPT1**, **↓PRPF8**, Ras, **↓RPL4**, **↑RPLPO**, **↑RSU1**, snRNP, **↓SNRNP200**, Sos, **↓STXBP3**, **↓TCP1**, **↑TGFBI**, **↓YWHAB**	49	23	Cellular assembly and organization, RNA posttranscriptional modification, protein synthesis
3	**20s proteasome**, **26s Proteasome**, **Actin**, **↑ACTN2**, **Alpha Actinin**, **Alpha catenin**, **Calcineurin protein(s)**, **↓CAP1**, **↑CKMT2**, **↑CPT1B***, **↑CSRP3**, **ERK1/2**, **↓EZR**, **F Actin**, **↓HARS**, **Hsp27**, **Hsp70**, **↑HSPB1**, **↑IDH1**, **↓IDH2**, **↑MVP**, **↓OTUB1**, **↑PACSIN2**, **Proteasome PA700/20s**, **↓PSMA8**, PSMB, **↑PSMB1**, **↓PSMB6**, **↓PSMB7**, **↓PSMD6**, **↑RDX**, **Rho gdi**, **Rock**, **Ubiquitin**, **↑VIM**	40	20	Cancer, hematological disease, cellular assembly and organization
4	**↓ADSL**, **↓APOA1BP**, BCAS2, **↓C21orf33**, **↑CNDP2**, **↑CRYZ**, CYC1, **↑DNPEP**, **↓ECI2**, FAM21A/FAM21C, FKBP15, HERC5, **↓HINT2**, **↓IDH3B**, **↑ISOC1**, KIAA0196, **↑KIAA1033**, **↓MTHFD1**, MTHFD1L, **↑MURC**, PI4K2A, **↑PROSC**, REXO4, TXNRD1, **↑TXNRD2**, UBC, **↑UQCR10**, UQCR11, UQCRB, UQCRC1, UQCRC2, UQCRFS1, UQCRQ, VPS29, WASH1	30	16	Cellular function and maintenance, posttranslational modification, protein synthesis
5	8-Oxo-7-hydrodeoxyguanosine, **↓ACAT1**, **↓APOBEC2**, BAG4, **↓BCKDHB**, beta-estradiol, Ces, **↓Ces1C***, **↑Ces1d**, CPT1, **↓CPT2**, **↑CPT1B***, EIF2AK1, **↑GC**, HERC5, IL6, **↑Kng1/Kng1I1**, **↑LUM**, MAO, neuroprotectin D1, **↓NID1**, NLRP12, NR1I2, **↓OXCT1**, PDYN, PHLDA1, **↓PMPCA**, PRSS23, **↑Rrbp1**, TM4SF1, TNF, TP53, triacylglycerol lipase, TXNRD1, UNG	24	14	Gene expression, cell cycle, cell death and survival
6	**↓4732456N10Rik**, **↓Adssl1**, caspase, CBLB, Collagen type I, copper, DMD, ERK, **↓ESD**, FBXO32, FSH, GAS6, GNRH, GRB2, GZMA, homocysteine, HSPB6, Jnk, lipoxin A4, MAOB, MAPKAPK5, MERTK, MYBPC3, **↓MYH4**, P2RX7, P38 MAPK, PDYN, **↑PGM5**, PI3K (complex), pyruvaldehyde, SERPINB2, **↑SERPINF1**, sorbitol, **↓THOP1**, Vegf	10	7	Free radical scavenging, cell death and survival, cell-to-cell signaling and interaction

[a] Data in bold denote focus proteins that were successfully mapped in the Ingenuity Pathway Knowledge Base.
[b] A score of >2 was considered significant ($p < 0.01$).

Those SNX rats treated with enalapril demonstrated less cardiac hypertrophy.

3.2. Cardiac structural and functional alteration

Fig. 1 illustrates the representative left ventricle blood pressure signals acquired from control rats, SNX rats treated with vehicle, and SNX rats treated with ACEi. Compared to SO controls, SNX rats had significantly higher left ventricular systolic pressure, which could be lowered by enalapril treatment.

SNX rats demonstrated a similar heart rate and systolic function (indexed by dP/dt_{max}, ejection fraction, and cardiac output) when compared with sham controls (Table 1). However, there was impaired diastolic function as shown by the decreased dP/dt_{min} and increased isovolumetric relaxation time. Compared with SNX rats receiving vehicle dosing, AECi treatment tended to improve diastolic function.

3.3. Comparative proteomics and pathway analysis

Compared to SO rats, SNX rats had 25 upregulated and 46 decreased protein expressions in the left ventricle. The top canonical pathways that participated in CKD cardiomyopathy were mitochondrial dysfunction, oxidative phosphorylation, fatty acid β oxidation, protein ubiquitination, and ketolysis (Fig. 2). From a total of nine overlapping networks generated by ingenuity pathway analysis (Ingenuity Systems; www.ingenuity.com), six had a score >10 (score ≥2 is significant; it represents the log of the probability that the network was found by chance) (Table 2). The most relevant functions extracted from these networks contained 27 and 23 focused proteins, respectively (Fig. 3). They were related to cellular assembly and organization, RNA posttranscriptional modification, and protein synthesis (Table 2).

Compared to SO rats, SNX rats treated with enalapril for with 6 weeks had 21 upregulated and 40 decreased protein expressions in the left ventricle. The residual canonical pathways mediating the CKD-related cardiomyopathy were mitochondrial dysfunction, ketolysis, phenylalanine degradation IV, and putrescine degradation III (Fig. 4). The most relevant functions extracted from the top two networks contained 24 and 15 focused proteins, respectively (Fig. 5). They were related to cellular assembly and organization, free radical scavenging, and renal damage (Table 3). Compared to SO rats for the most differentially expressed left ventricular proteins, there was a markedly decreased sirt3 and SNRNP200, and increased monoamine oxidase (MAO) and adenosylhomocysteinase (AHCY) for SNX rats treated with enalapril.

3.4. Western blot analysis

Expressions of Sirt3, SNRNP, MAO, and SAHH of the left ventricles from SO, SNX + vehicle, and SNX + enalapril rats were further validated by Western blot analysis (Fig. 6). Concordant with the proteomic findings, there was decreased expression of Sirt3 and SNRNP. However, there was also

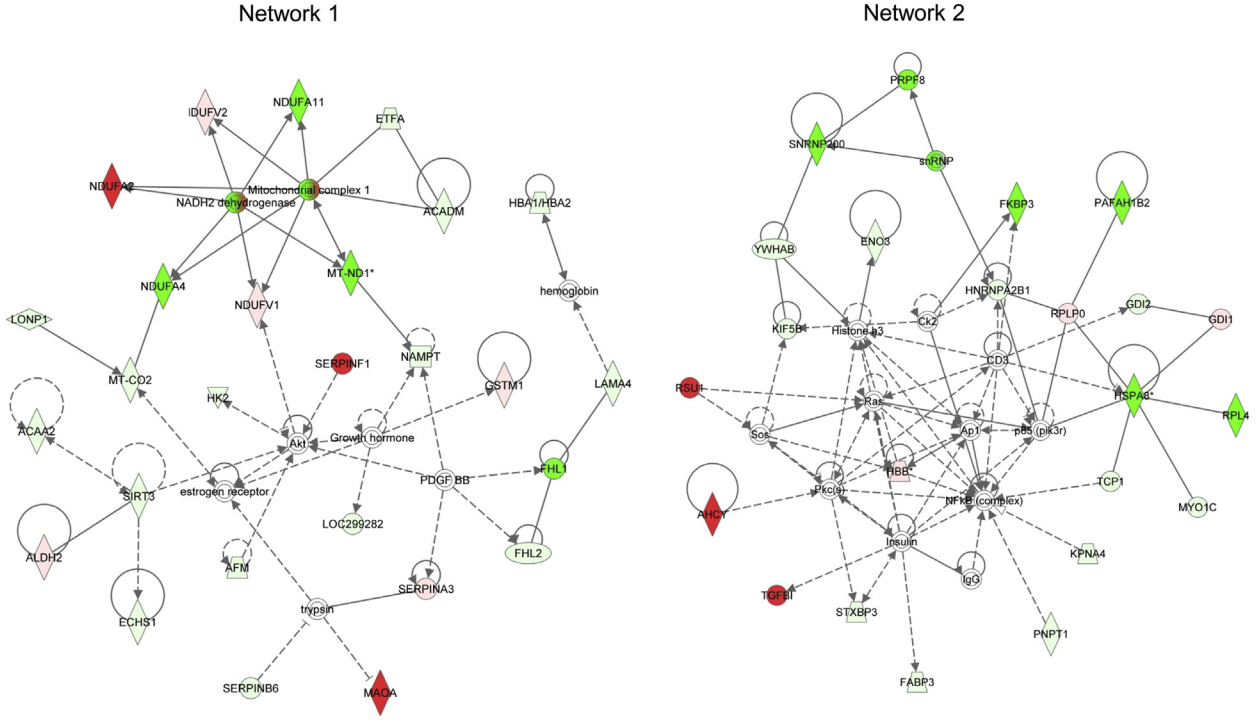

Fig. 3. Ingenuity pathway network 1 (score 61) and network 2 (score 49) based on the differentially expressed left ventricular proteins between the sham-operated rats and the subtotal nephrectomy rats treated with vehicle. Protein nodes with colored background are the identified proteins. Nodes with clear background are the interacting proteins added from the Ingenuity database. Unbroken lines connecting the proteins indicate direct interactions, and broken lines indicate indirect interactions.

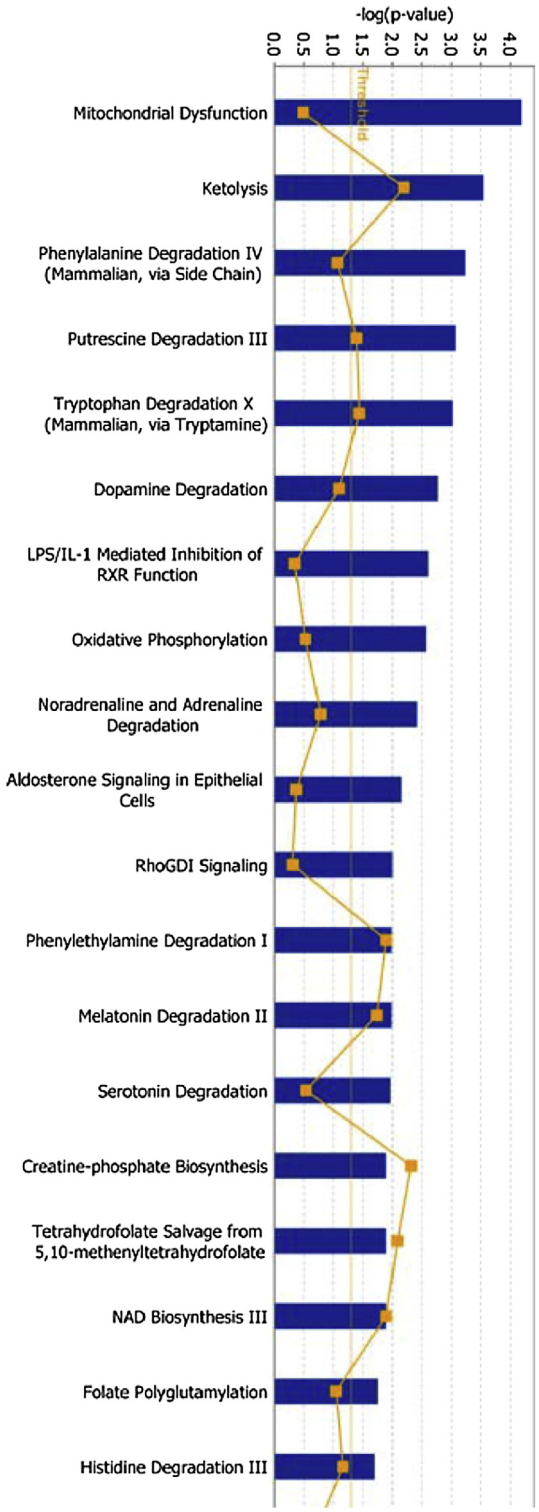

Fig. 4. Predominant canonical pathway identified by ingenuity pathway analysis for the differentially expressed left ventricular proteins between subtotal nephrectomy rats treated with enalapril and the sham-operated rats. The residual canonical pathways mediating the CKD-related cardiomyopathy are mitochondrial dysfunction, ketolysis, phenylalanine degradation IV, and putrescine degradation III. CKD = chronic kidney disease.

increased MAO and SAHH expression in renal dysfunctional status, which could not be ameliorated by enalapril.

4. Discussion

In the present study, we used the CKD model of SNX rats to investigate the alterations of left ventricular structure function in renal impairment status, and to evaluate the therapeutic effects of RAAS blockade by ACEi. We observed preserved systolic function and impaired diastolic function in SNX, which resembles the heart failure with preserved ejection fraction[11] found in CKD patients. ACEi cannot fully reverse the LV structural and functional derangements in CKD. Proteomic analysis of the SNX left ventricle revealed deranged functional pathways related to mitochondrial dysfunction, fatty acid β oxidation, protein ubiquitination, RNA posttranscriptional modification, and ketolysis. Again, ACEi could not thoroughly correct these irregularities. We observed markedly decreased sirt3 and SNRNP200, and increased MAO and AHCY in the left ventricles of enalapril-treated SNX rats, which could be promising candidates for multiple-target therapy.

4.1. SIRT3

We observed decreased *Sirt3* and *NAMPT* in the SNX heart, which could not be reversed by ACEi. Sirtuins are class III histones that necessitate nicotinamide adenine dinucleotide (NAD) for their activity with deacetylases. *Sirt3* governs the substrate for myocardial energy utilization by activating enzymes implemented in tricarboxylic acid cycle, fatty acid β oxidation, and ketogenesis. Therefore, *Sirt3* played a pivotal role in cardiac hypertrophy, a state that the substrate for myocardial energy utilization switches from fatty acid β oxidation to glycolysis. *Sirt3* also exerts cardioprotective effects by activating the Foxo3a-dependent antioxidant defense mechanism that scavenges cellular reactive oxygen species (ROS) and prevents cardiac hypertrophy.[12] *NAMPT* is a stress and nutrient-responsive protein that participates in the biosynthesis of NAD, which is responsible for the activity of sirtuins. Exogenous NAD has been shown to activate AMP-activated protein kinase, to rescue the heart from ATP depletion, stimulate PGC1α, and block the cardiac hypertrophic response.[13] We speculate that identifying drugs or nutrients (e.g., NAD supplementations) capable of increasing *Sirt3* expression or activity might be an attractive strategy to ameliorate CKD-related cardiomyopathy.[14]

4.2. SNRNP200

In the SNX LV, we observed decreased expression of SNRNP200 helicase and PRPF8, which are the major components of spliceosome. The spliceosome is composed of five small nuclear ribonucleoproteins and hundreds of proteins. It plays a crucial role in alternative splicing of premessenger RNAs by recognizing the intron/exon boundaries, catalyzing the removal of introns, and joining of exons. Through

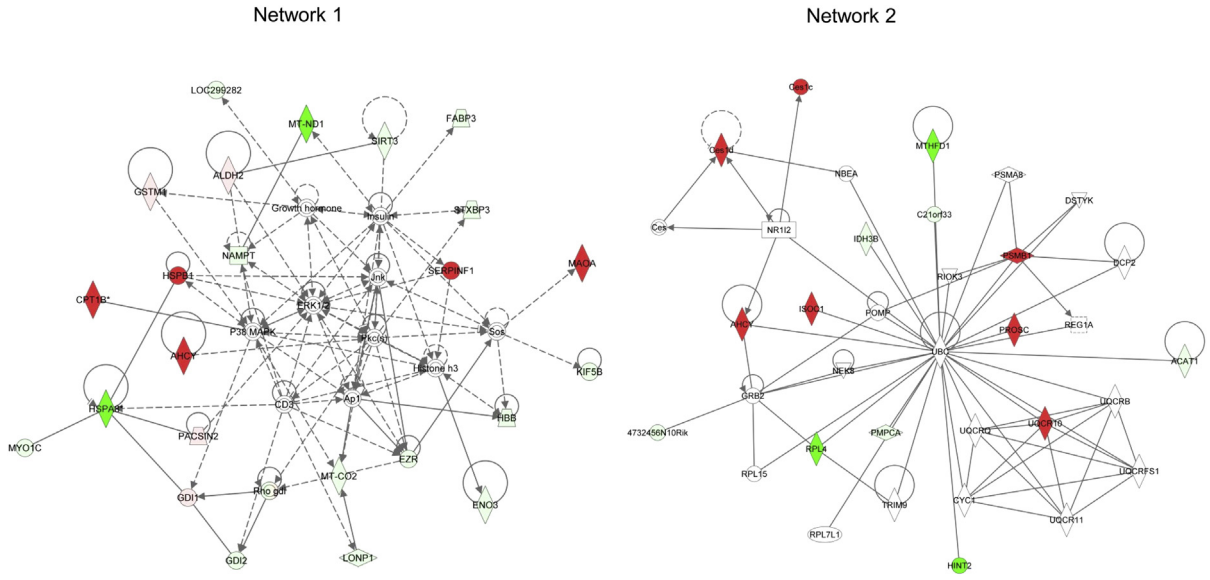

Fig. 5. Ingenuity pathway network 1 (score 61) and network 2 (score 33) based on the differentially expressed left ventricular proteins between subtotal nephrectomy rats treated with enalapril and the sham-operated rats. Protein nodes with colored background are the identified proteins. Nodes with clear background are the interacting proteins added from the Ingenuity database. Unbroken lines connecting the proteins indicate direct interactions, and broken lines indicate indirect interactions.

alternative splicing of the precursor transcripts, various mature mRNAs are produced and subsequently translated into functionally diverse protein isoforms from a single gene. Deranged exon exclusion, intron retention, or the use of alternative splice sites could significantly influence the protein structure, localization, regulation, and function. Disturbed expression of U5 small nuclear ribonucleoprotein associated U5-200kD RNA helicase could also cause cell cycle abnormalities.[15] Alternative splicing of sarcomeric genes, ion channels, and cell signaling proteins can lead to cardiomyopathies, arrhythmias, and other pathologies.[16] Based on the decreased expression of components in spliceosome, further studies are warranted to unravel the role of alternative splicing and RNA targets in the pathogenesis of CKD cardiomyopathy.

Table 3
Ingenuity pathway analysis of the differentially expressed left ventricular proteins of subtotal nephrectomy rats treated with enalapril when compared with the sham-operated rats.

ID	Molecules in network[a]	Score[b]	Focus molecule	Top diseases and functions
1	**↑AHCY**, **↑ALDH2**, Ap1, CD3, **↑CPT1B***, **↓ENO3**, ERK1/2, **↓EZR**, **↓FABP3**, **↑GDI1**, **↓GDI2**, Growth hormone, **↑GSTM1**, ↓HBB, Histone h3, **↓HSPA8***, **↑HSPB1**, Insulin, Jnk, **↓KIF5B**, **↓LOC299282**, **↓LONP1**, **↑MAOA**, **↓MT-CO2**, **↓MT-ND1**, **↓MYO1C**, **↓NAMPT**, P38 MAPK, **↑PACSIN2**, Pkc(s), Rho gdi, **↑SERPINF1**, **↓SIRT3**, Sos, **↓STXBP3**	61	24	Cellular assembly and organization, free radical scavenging, renal damage
2	**↓4732456N10Rik**, **↓ACAT1**, **↑AHCY**, **↓C21orf33**, **↑Ces1C**, **↑Ces1d**, CYC1, DCP2, DSTYK, GRB2, **↓HINT2**, **↓IDH3B**, **↑ISOC1**, **↓MTHFD1**, NBEA, NEK8, NR1I2, **↓PMPCA**, POMP, **↑PROSC**, PSMA8, **↑PSMB1**, REG1A, RIOK3, **↓RPL4**, RPL15, RPL7L1, TRIM9, UBC, **↑UQCR10**, UQCR11, UQCRB, UQCRFS1, UQCRQ	33	15	Cardiovascular disease, hereditary disorder, neurological disease
3	**↓Adssl1**, **↓AFM**, Akt, BAG4, beta-estradiol, **↑CKMT2**, **↑CRYZ**, DMD, DNAJC3, ENaC, FBXO32, Fe^{2+}, HRAS, **↑HSPB1**, HSPB6, HSPB8, HTR1A, IgG, IRAK2, KCND3, LAMP2, lipoxin A4, MTDH, **↓MYH4**, NFkB (complex), **↓NID1**, **↓OTUB1**, **↓OXCT1**, p85 (pik3r), PI3K (complex), PRSS23, RPL14, **↑RPLPO**, SERP1, sorbitol	20	10	Cardiac necrosis/cell death, cardiovascular system development and function, cell death and survival
4	**↓APOBEC2**, BCAS2, CD2BP2, CRNKL1, ECD, EFTUD2, EIF4E2, **↓LAMA4**, LSM4, NAA38, PLRG1, PPIH, PRPF3, PRPF4, PRPF6, **↓PRPF8**, PRPF31, PRPF4B, RBM5, RNU4-1, RNU5A-1, SART1, **↓SERPINB6**, SF3B4, SLU7, SMNDC1, SNRNP27, SNRNP40, **↓SNRNP200**, SNRPE, SNRPG, TOE1, TP53, USP39, **↓YWHAB**	10	6	RNA posttranscriptional modification, hereditary disorder, ophthalmic disease

[a] Data in bold denote focus proteins that were successfully mapped in the Ingenuity Pathway Knowledge Base.
[b] A score of >2 was considered significant ($p < 0.01$).

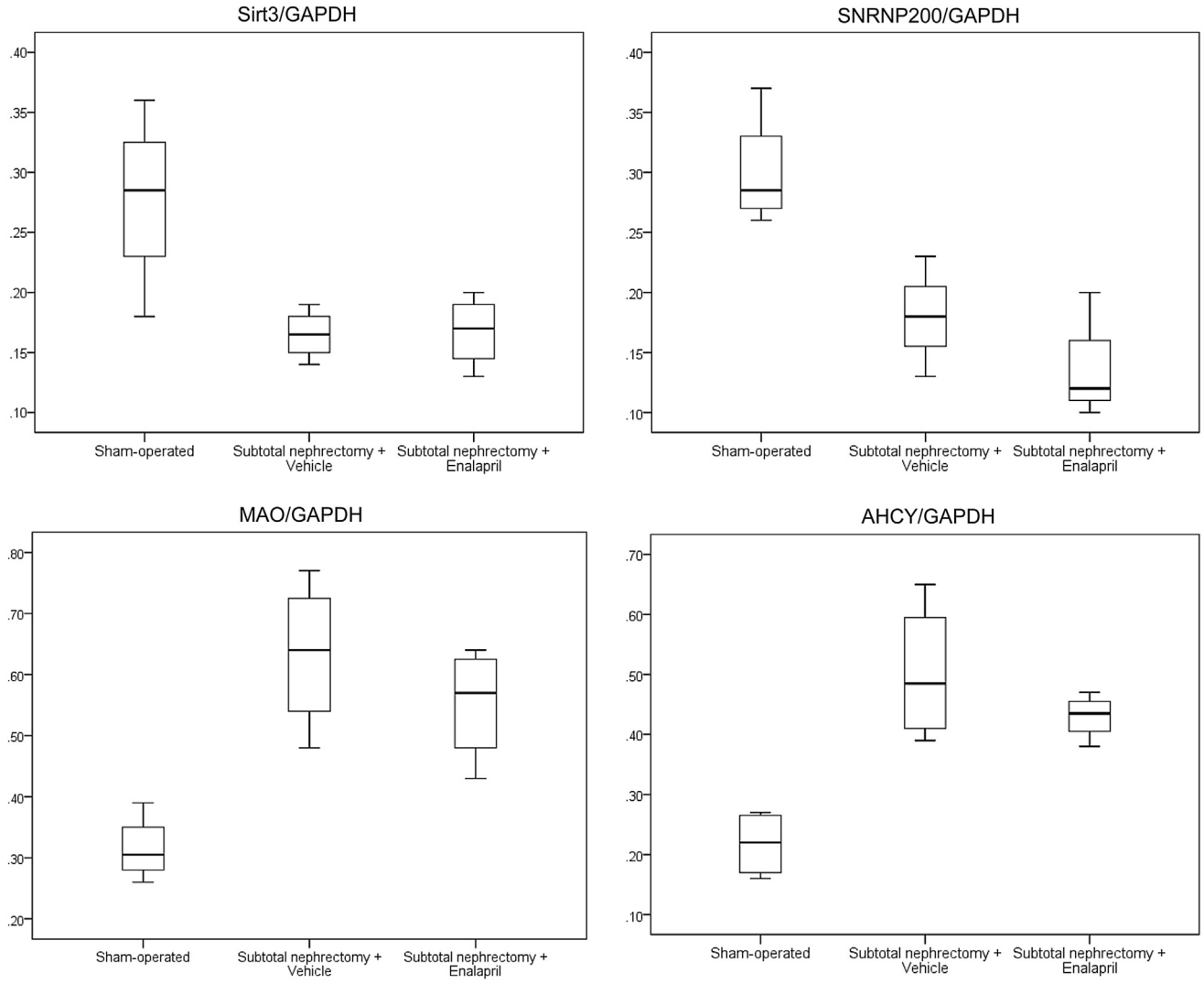

Fig. 6. Western blot validations of the differential expression of Sirt3, SNRNP200, MAO, and AHCY in the left ventricles of sham-operated rats, subtotal nephrectomy rats treated with vehicle, and those treated with enalapril. Concordant with the proteomic findings, there were decreased Sirt3 and SNRNP and increased MAO and SAHH expression in renal dysfunctional status, which could not be ameliorated by enalapril. AHCY = adenosylhomocysteinase; MAO = monoamine oxidase.

4.3. MAO

MAOs are the flavoenzymes located at the outer membrane of mitochondria, which are the major sources of ROS in cardiomyocytes.[17] They are responsible for the oxidative deamination of catecholamines, serotonin, and biogenic amines. During the process of MAO-mediated deamination, the by-product as aldehydes could be deleterious to the heart by deactivating proteasomes and altering mitochondrial bioenergetics.[18] Therefore, there are intricate connections among MAO activation, mitochondrial ROS formation, and mitochondrial dysfunction,[19] all of which are involved in myocardial degeneration in heart failure and aging.[20] Remarkably, several transcriptomic or proteomic studies have already identified upregulated MAO-A in experimental rat heart failure models of volume overload,[21] pressure overload,[22] and myocardial infarction,[23] and suppression of myocardial MAO has displayed beneficial effects. *In vitro* studies have shown that senescent cardiomyocytes exhibited distinctly enhanced MAO-A activity, and cardiomyocytes exposed to angiotensin II displayed marked MAO activation.[24] Given that CKD is a status of enhanced RAAS activation reflected by increased angiotensin II[25] and accelerated senescence,[26] and that CKD cardiomyopathy is the combination of pressure and volume overloads,[27] we think that MAO inhibition might be promising for alleviating cardiac pathologies.

4.4. AHCY

S-Adenosylhomocysteine hydrolase (AHCY) catalyzes the hydrolysis of *S*-adenosylhomocysteine to homocysteine and adenosine,[28] which is the only source of homocysteine in mammals. Increased AHCY expressions were detected in our study, particularly in the SNX left ventricles that denote the increased homocysteine generation *in situ*. Homocysteine could induce endothelial dysfunction through the decreased

bioavailability of nitric oxide and increased oxidative stress on vasculature causing thrombosis liability. It could also injure cardiomyocytes through the activation of p38 MAPK, decreased expression of thioredoxin, and increased ROS production, ultimately leading to impaired cardiomyocyte contractility and apoptosis.[29] Hyperhomocysteinemia is the well-recognized risk factor for cardiovascular complications in CKD.[30] However, several RCTs aimed to decrease the blood homocysteine level failed to render improved clinical outcomes. We reasoned that lower blood homocysteine does not necessarily reflect the real tissue concentration in CKD left ventricles. It would be innovative to evaluate whether suppressing AHCY activity would be beneficial to cardiac hypertrophy.

4.5. Others

Several other potential proteins may merit further evaluation. The SNX rats had an increased expression of MURC (muscle-restricted coiled-coil protein), a member of the caveolin family,[31] which is the hypertrophy-regulated gene that increases myocardial expression under pressure overload.[32] It modulates the rho/rock pathway, and induces cardiac dysfunction and conduction disturbance. There is decreased FHL2 in the SNX left ventricle in the present study. FHL2 functions to suppress calcineurin signaling and NFAT (nuclear factor of activated T cell) activation, and consequently inhibits pathological cardiac growth.[33] Actually, decreased FHL2 expression is also observed in failing human hearts.[34] Moreover, we also found decreased FABP3 (heart-type fatty acid binding protein-3), which is a cytosolic fatty acid shuttle that facilitates the movement of fatty acids in cardiac muscle. It reversibly binds and moves fatty acids from the plasma membrane into storage or to the mitochondria for oxidation. Decreased FABP3 expression might hamper cardiac fatty acid utilization and increase the dependence on glucose as a substrate.

In conclusion, consistent with previous clinical reports, we observed that simply using the RAAS blockade by ACEi could not untangle the intricate pathways involved in CKD-related cardiomyopathy in this animal study. Further comprehensive investigations of these pathways and the renocardiac network would facilitate the development of a multifaceted intervention for clinical applications in the future.

Acknowledgments

This work was supported in part by grants (NSC 100-2314-B-075-080 and NSC 102-2314-B-075 -060) from the Ministry of Science and Technology, Taiwan, and grants (V96ER3-003, V99ER3-008, VGHUST100-G7-5-1, VGHUST100-G7-5-3, and V102C-170) from the Taipei Veterans General Hospital in Taiwan. This work was assisted in part by the Division of Experimental Surgery of the Department of Surgery, Taipei Veterans General Hospital. The authors are grateful for the facility provided by the Core Laboratory (Taipei, Taiwan) for Junior Clinical Physicians.

References

1. Samuels JA, Molony DA. Randomized controlled trials in nephrology: state of the evidence and critiquing the evidence. *Adv Chronic Kidney Dis* 2012;**19**:40–6.
2. Decker E, Kendrick J. Research in the CKD clinic: highs and lows. *Adv Chronic Kidney Dis* 2014;**21**:344–8.
3. Mancia G, De Backer G, Dominiczak A, Cifkova R, Fagard R, Germano G, et al. 2007 Guidelines for the Management of Arterial Hypertension: the Task Force for the Management of Arterial Hypertension of the European Society of Hypertension (ESH) and of the European Society of Cardiology (ESC). *J Hypertens* 2007;**25**:1105–87.
4. Sharma P, Blackburn RC, Parke CL, McCullough K, Marks A, Black C. Angiotensin-converting enzyme inhibitors and angiotensin receptor blockers for adults with early (stage 1 to 3) non-diabetic chronic kidney disease. *Cochrane Database Syst Rev* 2011:CD007751.
5. Chang TI, Shilane D, Brunelli SM, Cheung AK, Chertow GM, Winkelmayer WC. Angiotensin-converting enzyme inhibitors and cardiovascular outcomes in patients on maintenance hemodialysis. *Am Heart J* 2011;**162**:324–30.
6. Dyadyk AI, Bagriy AE, Lebed IA, Yarovaya NF, Schukina EV, Taradin GG. ACE inhibitors captopril and enalapril induce regression of left ventricular hypertrophy in hypertensive patients with chronic renal failure. *Nephrol Dial Transplant* 1997;**12**:945–51.
7. Yu WC, Lin YP, Lin IF, Chuang SY, Chen CH. Effect of ramipril on left ventricular mass in normotensive hemodialysis patients. *Am J Kidney Dis* 2006;**47**:478–84.
8. Lam MP, Vivanco F, Scholten A, Hermjakob H, Van Eyk J, Ping P. HUPO 2011: the new Cardiovascular Initiative — integrating proteomics and cardiovascular biology in health and disease. *Proteomics* 2012;**12**:749–51.
9. Lin YP, Hsu ME, Chiou YY, Hsu HY, Tsai HC, Peng YJ, et al. Comparative proteomic analysis of rat aorta in a subtotal nephrectomy model. *Proteomics* 2010;**10**:2429–43.
10. Liao CC, Chen YW, Jeng TL, Li CR, Kuo CF. Consumption of purple sweet potato affects post-translational modification of plasma proteins in hamsters. *J Agric Food Chem* 2013;**61**:12450–8.
11. Sharma K, Kass DA. Heart failure with preserved ejection fraction: mechanisms, clinical features, and therapies. *Circ Res* 2014;**115**:79–96.
12. Sundaresan NR, Gupta M, Kim G, Rajamohan SB, Isbatan A, Gupta MP. Sirt3 blocks the cardiac hypertrophic response by augmenting Foxo3a-dependent antioxidant defense mechanisms in mice. *J Clin Invest* 2009;**119**:2758–71.
13. Pillai VB, Sundaresan NR, Kim G, Gupta M, Rajamohan SB, Pillai JB, et al. Exogenous NAD blocks cardiac hypertrophic response via activation of the SIRT3–LKB1–AMP-activated kinase pathway. *J Biol Chem* 2010;**285**:3133–44.
14. Giralt A, Villarroya F. SIRT3, a pivotal actor in mitochondrial functions: metabolism, cell death and aging. *Biochem J* 2012;**444**:1–10.
15. Ehsani A, Alluin JV, Rossi JJ. Cell cycle abnormalities associated with differential perturbations of the human U5 snRNP associated U5-200kD RNA helicase. *PLoS One* 2013;**8**:e62125.
16. Lara-Pezzi E, Gomez-Salinero J, Gatto A, Garcia-Pavia P. The alternative heart: impact of alternative splicing in heart disease. *J Cardiovasc Transl Res* 2013;**6**:945–55.
17. Balaban RS, Nemoto S, Finkel T. Mitochondria, oxidants, and aging. *Cell* 2005;**120**:483–95.
18. Chen CH, Sun L, Mochly-Rosen D. Mitochondrial aldehyde dehydrogenase and cardiac diseases. *Cardiovasc Res* 2010;**88**:51–7.
19. Kaludercic N, Carpi A, Nagayama T, Sivakumaran V, Zhu G, Lai EW, et al. Monoamine oxidase B prompts mitochondrial and cardiac dysfunction in pressure overloaded hearts. *Antioxid Redox Signal* 2014;**20**:267–80.
20. Villeneuve C, Guilbeau-Frugier C, Sicard P, Lairez O, Ordener C, Duparc T, et al. p53-PGC-1alpha pathway mediates oxidative mitochondrial damage and cardiomyocyte necrosis induced by monoamine oxidase-A upregulation: role in chronic left ventricular dysfunction in mice. *Antioxid Redox Signal* 2013;**18**:5–18.

21. Petrak J, Pospisilova J, Sedinova M, Jedelsky P, Lorkova L, Vit O, et al. Proteomic and transcriptomic analysis of heart failure due to volume overload in a rat aorto-caval fistula model provides support for new potential therapeutic targets — monoamine oxidase A and transglutaminase 2. *Proteome Sci* 2011;**9**:69.
22. Kaludercic N, Takimoto E, Nagayama T, Feng N, Lai EW, Bedja D, et al. Monoamine oxidase A-mediated enhanced catabolism of norepinephrine contributes to adverse remodeling and pump failure in hearts with pressure overload. *Circ Res* 2010;**106**:193−202.
23. Lancaster TS, Jefferson SJ, Hunter JC, Lopez V, Van Eyk JE, Lakatta EG, et al. Quantitative proteomic analysis reveals novel mitochondrial targets of estrogen deficiency in the aged female rat heart. *Physiol Genomics* 2012;**44**:957−69.
24. Manni ME, Zazzeri M, Musilli C, Bigagli E, Lodovici M, Raimondi L. Exposure of cardiomyocytes to angiotensin II induces over-activation of monoamine oxidase type A: implications in heart failure. *Eur J Pharmacol* 2013;**718**:271−6.
25. Ruggenenti P, Cravedi P, Remuzzi G. Mechanisms and treatment of CKD. *J Am Soc Nephrol* 2012;**23**:1917−28.
26. Stenvinkel P, Larsson TE. Chronic kidney disease: a clinical model of premature aging. *Am J Kidney Dis* 2013;**62**:339−51.
27. Taddei S, Nami R, Bruno RM, Quatrini I, Nuti R. Hypertension, left ventricular hypertrophy and chronic kidney disease. *Heart Fail Rev* 2011;**16**:615−20.
28. Baric I, Fumic K, Glenn B, Cuk M, Schulze A, Finkelstein JD, et al. *S*-Adenosylhomocysteine hydrolase deficiency in a human: a genetic disorder of methionine metabolism. *Proc Natl Acad Sci U S A* 2004;**101**:4234−9.
29. Wang X, Cui L, Joseph J, Jiang B, Pimental D, Handy DE, et al. Homocysteine induces cardiomyocyte dysfunction and apoptosis through p38 MAPK-mediated increase in oxidant stress. *J Mol Cell Cardiol* 2012;**52**:753−60.
30. Robinson K. Renal disease, homocysteine, and cardiovascular complications. *Circulation* 2004;**109**:294−5.
31. Bastiani M, Liu L, Hill MM, Jedrychowski MP, Nixon SJ, Lo HP, et al. MURC/Cavin-4 and cavin family members form tissue-specific caveolar complexes. *J Cell Biol* 2009;**185**:1259−73.
32. Ogata T, Ueyama T, Isodono K, Tagawa M, Takehara N, Kawashima T, et al. MURC, a muscle-restricted coiled-coil protein that modulates the Rho/ROCK pathway, induces cardiac dysfunction and conduction disturbance. *Mol Cell Biol* 2008;**28**:3424−36.
33. Hojayev B, Rothermel BA, Gillette TG, Hill JA. FHL2 binds calcineurin and represses pathological cardiac growth. *Mol Cell Biol* 2012;**32**:4025−34.
34. Bovill E, Westaby S, Crisp A, Jacobs S, Shaw T. Reduction of four-and-a-half LIM-protein 2 expression occurs in human left ventricular failure and leads to altered localization and reduced activity of metabolic enzymes. *J Thorac Cardiovasc Surg* 2009;**137**:853−61.